RESEARCH BRIEF

TCR Repertoire Intratumor Heterogeneity in Localized Lung Adenocarcinomas: An Association with Predicted Neoantigen Heterogeneity and Postsurgical Recurrence

Alexandre Reuben[1,2], Rachel Gittelman[3], Jianjun Gao[4], Jiexin Zhang[5], Erik C. Yusko[3], Chang-Jiun Wu[2], Ryan Emerson[3], Jianhua Zhang[2], Christopher Tipton[3], Jun Li[2], Kelly Quek[2,6], Vancheswaran Gopalakrishnan[1], Runzhe Chen[2,6], Luis M. Vence[7], Tina Cascone[6], Marissa Vignali[3], Junya Fujimoto[8], Jaime Rodriguez-Canales[8], Edwin R. Parra[8], Latasha D. Little[2], Curtis Gumbs[2], Marie-Andrée Forget[9], Lorenzo Federico[9], Cara Haymaker[9], Carmen Behrens[8], Sharon Benzeno[3], Chantale Bernatchez[9], Boris Sepesi[10], Don L. Gibbons[6], Jennifer A. Wargo[1,2], William N. William Jr[6], Stephen Swisher[10], John V. Heymach[6], Harlan Robins[3,11], J. Jack Lee[12], Padmanee Sharma[4,7], James P. Allison[7], P. Andrew Futreal[2], Ignacio I. Wistuba[8], and Jianjun Zhang[2,6]

ABSTRACT

Genomic intratumor heterogeneity (ITH) may be associated with postsurgical relapse of localized lung adenocarcinomas. Recently, mutations, through generation of neoantigens, were shown to alter tumor immunogenicity through T-cell responses. Here, we performed sequencing of the T-cell receptor (TCR) in 45 tumor regions from 11 localized lung adenocarcinomas and observed substantial intratumor differences in T-cell density and clonality with the majority of T-cell clones restricted to individual tumor regions. TCR ITH positively correlated with predicted neoantigen ITH, suggesting that spatial differences in the T-cell repertoire may be driven by distinct neoantigens in different tumor regions. Finally, a higher degree of TCR ITH was associated with an increased risk of postsurgical relapse and shorter disease-free survival, suggesting a potential clinical significance of T-cell repertoire heterogeneity.

SIGNIFICANCE: The present study provides insights into the ITH of the T-cell repertoire in localized lung adenocarcinomas and its potential biological and clinical impact. The results suggest that T-cell repertoire ITH may be tightly associated to genomic ITH and disease relapse. *Cancer Discov; 7(10); 1088–97. ©2017 AACR.*

[1]Department of Surgical Oncology, The University of Texas MD Anderson Cancer Center, Houston, Texas. [2]Department of Genomic Medicine, The University of Texas MD Anderson Cancer Center, Houston, Texas. [3]Adaptive Biotechnologies, Seattle, Washington. [4]Department of Genitourinary Medical Oncology, The University of Texas MD Anderson Cancer Center, Houston, Texas. [5]Department of Bioinformatics and Computational Biology, The University of Texas MD Anderson Cancer Center, Houston, Texas. [6]Department of Thoracic/Head and Neck Medical Oncology, The University of Texas MD Anderson Cancer Center, Houston, Texas. [7]Department of Immunology, The University of Texas MD Anderson Cancer Center, Houston, Texas. [8]Department of Translational Molecular Pathology, The University of Texas MD Anderson Cancer Center, Houston, Texas. [9]Department of Melanoma Medical Oncology, The University of Texas MD Anderson Cancer Center, Houston, Texas. [10]Department of Thoracic Surgical Oncology, The University of Texas MD Anderson Cancer Center, Houston, Texas. [11]Department of Computational Biology, Fred Hutchinson Cancer Research Center, Seattle, Washington. [12]Department of Biostatistics, The University of Texas MD Anderson Cancer Center, Houston, Texas.

Note: Supplementary data for this article are available at Cancer Discovery Online (http://cancerdiscovery.aacrjournals.org/).

Current address for C. Tipton: Department of Immunology, Emory University, Atlanta, GA.

Corresponding Authors: Jianjun Zhang, The University of Texas MD Anderson Cancer Center, Unit 432, 1515 Holcombe Boulevard, Houston, TX 77030. Phone: 713-792-0056; E-mail: jzhang20@mdanderson.org; Ignacio I. Wistuba, iiwistuba@mdanderson.org; and P. Andrew Futreal, afutreal@mdanderson.org

doi: 10.1158/2159-8290.CD-17-0256

INTRODUCTION

Immune checkpoint blockade therapy targeting CTLA4, PD-1, and PD-L1 has shown substantial rates of durable clinical benefit in patients with various metastatic cancer types (1–6). However, response rates remain only 20% to 30% in an unselected patient population across different tumor histologies (2, 3, 7–11). The molecular mechanisms underlying resistance to immune checkpoint blockade are imperfectly understood and have been the focus of intense scrutiny in recent years. Importantly, although significant progress has been made, there are currently no optimal biomarkers to predict response to immune checkpoint blockade in non–small cell lung cancer (NSCLC). PD-L1 is the only approved biomarker for immune checkpoint blockade therapy with anti–PD-1, but the presence of robust responses in patients with low tumor PD-L1 expression argues against the value of PD-L1 as an exclusionary predictive biomarker (12). One of the explanations for this is the substantial intratumor heterogeneity (ITH)—specifically in regard to PD-L1 expression—observed in NSCLC (13).

We previously delineated the genomic ITH of localized lung adenocarcinomas by multiregion whole-exome sequencing (WES) and demonstrated that a higher level of genomic ITH was associated with an increased risk of relapse (14). More recently, McGranahan and colleagues showed that a higher proportion of heterogeneous predicted neoantigens was associated with an inferior response to CTLA4 and PD-1 immune checkpoint blockade in patients with NSCLC (15). Given that T-cell recognition is important for establishing an immune response to tumor-specific, mutation-derived neoantigens, these data warrant investigation of the T-cell repertoire in NSCLC.

T-cell receptor (TCR) sequencing is an emerging approach allowing characterization of the T-cell repertoire in an increasing number of studies (16). The reactivity of the TCRs expressed by tumor-infiltrating lymphocytes (TIL) determines their capacity to interact with tumor antigens presented on antigen-presenting cells (APC). Accordingly, the TCR repertoire has been reported to be associated with response to immune checkpoint blockade and survival in patients with cancer (16, 17). In the current study, we sought to assess the T-cell repertoire in the same 11 localized adenocarcinomas previously utilized to derive genomic ITH (14), in order to evaluate the T-cell landscape in the context of ITH and how it correlates with the genomic landscape and with patient outcome. Here, we report the characterization of this localized lung adenocarcinoma patient cohort through multiregion immunosequencing.

RESULTS

The Predicted Neoantigen Landscape Is Subject to ITH in Lung Adenocarcinomas

In light of our previous work identifying substantial mutational heterogeneity in lung adenocarcinomas, we first sought to determine whether the predicted neoantigen landscape mirrors the mutational landscape. To do so, we performed *in silico* prediction of HLA-A/B/C (MHC I) and HLA-DR/DQ (MHC II) neoantigens based on mutation data. In these analyses, we identified an average of 130 total (IC_{50} < 500 nmol/L) and 65 high-affinity (IC_{50} < 50 nmol/L) MHC I and 106 total and 9 high-affinity MHC II predicted neoantigens (Supplementary Fig. S1A–S1D). We next quantified the proportion of predicted branch neoantigens, defined as those *not* detected in all regions of a given tumor. This analysis revealed that between 1% (Patient #317) and 63% (Patient #356) of predicted MHC I neoantigens were on branches (Fig. 1A). Of particular interest, patients with disease recurrence presented a higher proportion of branch predicted neoantigens (Fig. 1B and C; ref. 14). These trends held true when investigating predicted MHC II neoantigens, with between 1% (Patient #317) and 47% (Patient #270) of predicted MHC II neoantigens found on branches and a similar association with patient recurrence (Fig. 1D–F).

Although numerous somatic mutations may be predicted to give rise to neoantigens, these may not be expressed. In order to filter out predicted neoantigens lacking expression in lung adenocarcinoma, we next queried gene expression data from The Cancer Genome Atlas (TCGA; ref. 18). In these analyses, we focused solely on predicted neoantigens in genes expressed above the median value and observed similar trends, though statistical significance was lost with MHC II neoantigens (Supplementary Fig. S2A–S2F).

ITH in T-cell Infiltrate and Clonality Is Observed in Lung Adenocarcinomas

Autoreactive T cells are deleted in the context of T-cell tolerance, supporting the premise that T cells may be reactive to neoantigens arising from tumor-derived nonsilent mutations. T cells are known to expand as a result of antigen recognition through their TCR, further strengthening the antitumor response. Therefore, to investigate the spatial heterogeneity of the TCR repertoire, we performed multiregion TCR profiling via ImmunoSEQ of 45 tumor regions (2 to 5 regions per tumor) from these 11 patients with localized lung adenocarcinomas (Supplementary Table S1). We obtained sequences from an average of 18,766 T cells per sample (ranging from 2,573 to 51,206). Within this total population of T cells, we observed an average of 8,400 unique TCRβ rearrangements per sample (ranging from 1,777 to 21,161).

We next evaluated the ITH in the density of T cells in each lung adenocarcinoma. These studies demonstrated that T-cell infiltrates represented on average between 4% (Patient #292) and 23% (Patient #472) of all nucleated cells (Fig. 2A). In order to investigate T-cell infiltrate ITH, we next quantified the T-cell density in multiple regions (2 to 5) within the same tumor. As shown in Fig. 2B, significant variation was observed across different regions of the same tumor when comparing the most and least infiltrated regions, with variations ranging between 11% (Patient #283) and 85% (Patient #270), suggesting variable ITH in T-cell infiltration in different tumors (Fig. 2C). Interestingly, this ITH extended to the number of unique TCR rearrangements detected in each region, suggesting differences not only in the total T-cell density, but also in the number of unique T-cell clones (Supplementary Fig. S3).

Next, we studied T-cell clonality, a metric of T-cell expansion, and reactivity, which ranges from 0 to 1 and describes

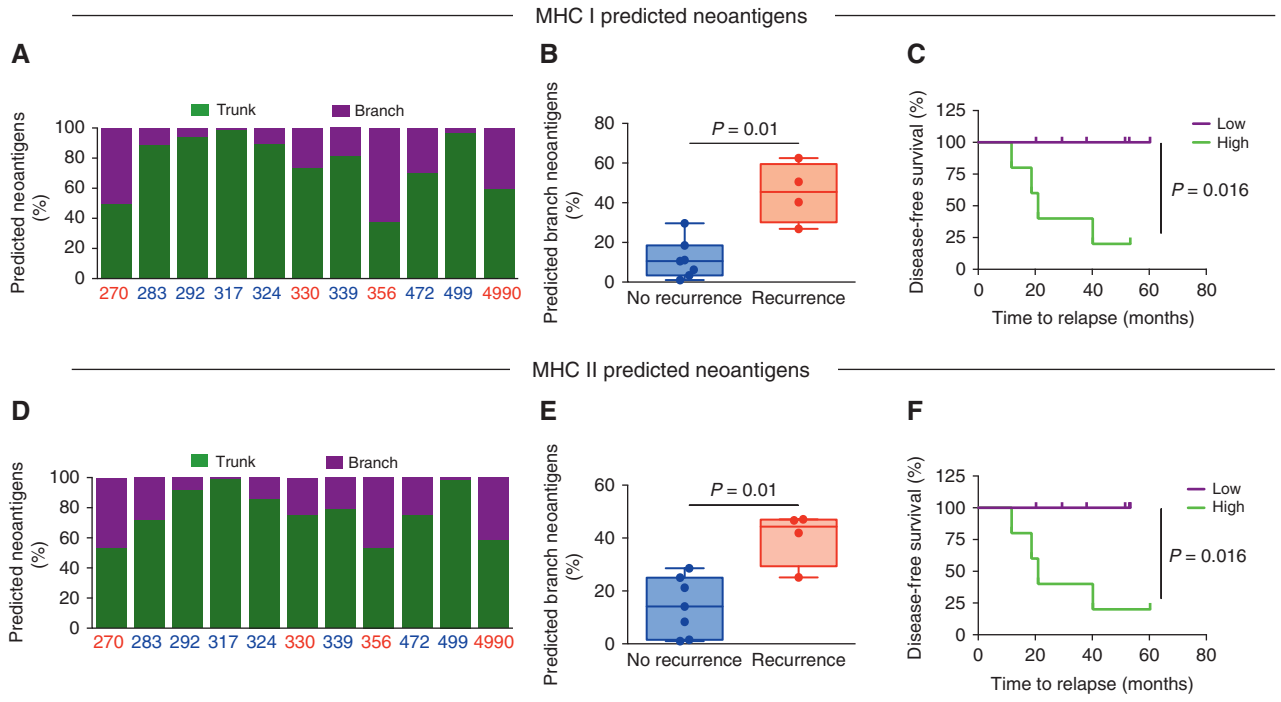

Figure 1. An increased proportion of branch predicted neoantigens in relapsed lung adenocarcinomas. **A,** Trunk (green) and branch (purple) predicted MHC I neoantigens in each patient. Red patient IDs = patients who relapsed; blue patient IDs = patients who have not relapsed. **B,** Comparison of percentage of branch predicted MHC I neoantigen burden in patients who relapsed (red) and patients who did not (blue). **C,** Disease-free survival in patients with high (green) and low (purple) percentage of predicted MHC I neoantigens. **D,** Trunk (green) and branch (purple) predicted MHC II neoantigens in each patient. Red patient IDs = patients who relapsed; blue patient IDs = patients who have not relapsed. **E,** Comparison of percentage of branch predicted MHC II neoantigen burden in patients who relapsed (red) and patients who did not (blue). **F,** Disease-free survival in patients with high (green) and low (purple) percentage of predicted MHC II neoantigens.

the shape of T-cell frequency distribution: Clonality values approaching 0 indicate a very even distribution of clone frequencies, whereas values approaching 1 indicate an increasingly asymmetric distribution in which a few clones are present at high frequencies. Analysis of T-cell clonality revealed that this metric ranged from 0.045 in Patient #292 to 0.169 in Patient #317 (Fig. 2D). Furthermore, ITH was observed in T-cell clonality in all tumors (Fig. 2E), with differences as large as 50% in T-cell clonality across different tumor regions in Patient #4990 (Fig. 2F). To focus on T-cell clones more likely to be relevant to the tumor, we profiled the TCR repertoire from available paired blood samples from 8 patients. We analyzed TCR rearrangements that were enriched in tumors compared with peripheral blood and recalculated T-cell density and clonality of these tumor-enriched T-cell clones. These analyses confirmed the substantial ITH in the TCR repertoire among tumor-enriched T-cell clones (Supplementary Fig. S4A–S4F).

TCR ITH Is Observed across Regions of the Same Tumor, but Limited among the Most Dominant T-cell Clones in Lung Adenocarcinomas

Considering the intratumor differences observed in T-cell frequency and clonality, we next investigated the overlap in T-cell clones across different regions from a same tumor. We first studied the overlap in the entire T-cell repertoire across different regions of each individual tumor. As shown in Fig. 3A and Supplementary Fig. S5, the vast majority of T-cell clones were restricted to individual tumor regions, with as little as 1% (Patient #4990) and at most 14% (Patient #356) of T-cell clones found in all regions of a single tumor, suggesting the presence of substantial ITH within the T-cell repertoire.

We then compared different tumor regions by looking exclusively at the top 5 most abundant T-cell clones in each patient. These analyses suggested that, in 64% of patients (7 of 11), the top clone in the patient remained most dominant in each region of the tumor, though its frequency did vary substantially. However, in the 4 remaining patients, the rank of the top clone varied greatly across regions, ranking as low as 12th in region T6 of Patient #4990 (Supplementary Fig. S6). Importantly, the top 5 clones were detectable in all regions of individual tumors, regardless of rank. Taken together, these data suggest potential differences in the immunogenicity of distinct regions within the same tumor, though the most reactive T cells were preserved across spatially distinct regions, potentially due to the conservation of the most immunogenic mutations across these regions in each tumor.

Variable TCR ITH Is Observed across Different Patients with NSCLC

To quantitatively assess the similarity and overlap between the T-cell repertoires in different samples and quantify the

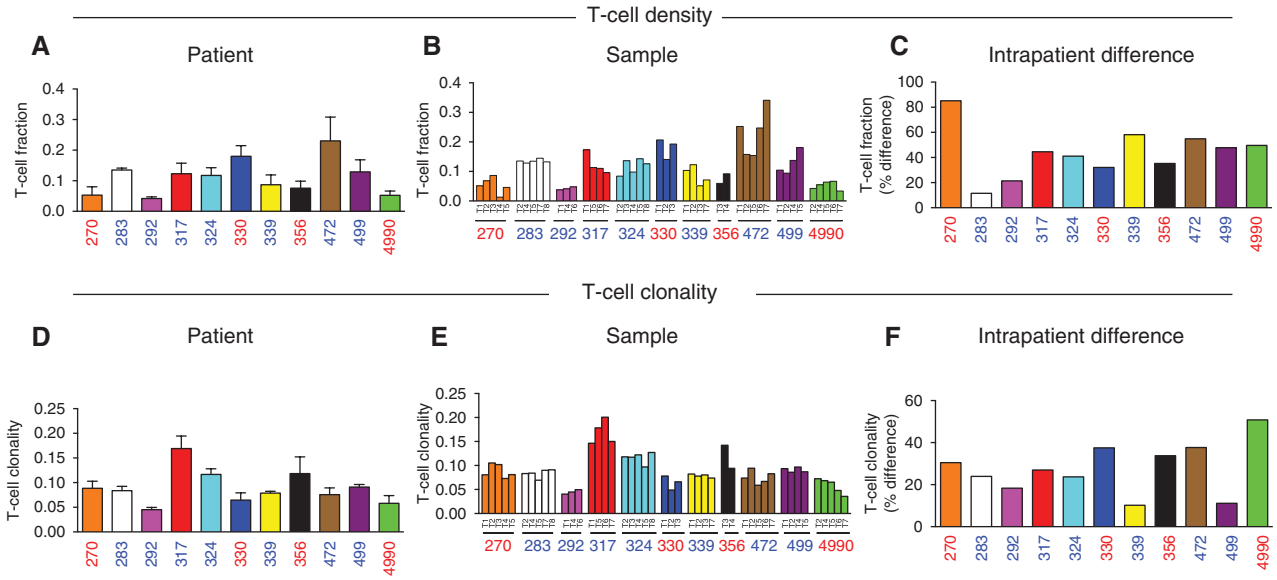

Figure 2. ITH in T-cell density and clonality in localized lung adenocarcinomas. **A,** Average T-cell density in each tumor as defined by ImmunoSeq. **B,** T-cell density in each tumor region. **C,** Maximal difference in T-cell density, defined as the difference between highest and lowest T-cell density across regions within the same tumor expressed as a percent difference. **D,** Average T-cell clonality in each patient as defined by ImmunoSeq. **E,** T-cell clonality in each tumor region. **F,** Maximal difference in T-cell clonality, defined as the difference between highest and lowest T-cell clonality across regions within the same tumor expressed as a percent difference. Red patient IDs = patients who relapsed; blue patient IDs = patients who have not relapsed.

TCR ITH, we utilized the Morisita overlap index (MOI), which takes into consideration the composition as well as the abundance of T-cell rearrangements. MOI ranges from 0 to 1, with 1 indicating identical TCR repertoires and 0 indicating completely distinct TCR repertoires between 2 samples. These results first confirmed a lack of overlap in the T-cell repertoire when comparing different patients with an MOI approaching 0, as expected. However, TCR repertoire ITH was evident in all patients, though its complexity varied with an MOI ranging from 0.48 to 0.98 across different regions (Fig. 3B). MOI was also calculated on tumor-enriched T cells compared with paired blood samples in the 8 patients whose blood samples were available and revealed a strong correlation between overall MOI and tumor-enriched MOI (Supplementary Fig. S7A–S7C). Taken together, these results demonstrate marked interindividual TCR repertoire heterogeneity and, to a lesser extent, intratumor TCR heterogeneity.

TILs in NSCLC Are Predominantly CD4-Positive

Though promising, TCR sequencing does not provide T-cell subtype information when performed on bulk tumor. Therefore, to determine the composition of the T-cell infiltrate, we next performed immune profiling by IHC. To do so, $CD3^+$, $CD4^+$, and $CD8^+$ T cells were quantified in 5 1-mm^2 regions within each tumor to evaluate the average density as a count of positive cells/mm^2. Consistent with our previous studies (19, 20), infiltrating T cells were found to have a CD4:CD8 T-cell ratio of 2.38:1 (ranging from 1.0 in Patient #330 to 3.55 in Patient #283; Supplementary Fig. S8A–S8C). Interestingly, despite employing different technologies, ITH in the T-cell density evaluated by ImmunoSeq correlated strongly with ITH in the $CD3^+$ T-cell density evaluated by IHC (Supplementary Fig. S8D). However, no correlation was observed between CD4, CD8, or CD4:CD8 ratio and patient relapse.

Higher ITH in the T-cell Repertoire Is Associated with a Higher Risk of Relapse

In light of our previous work suggesting a higher proportion of branch mutation correlates with increased risk of relapse, and considering the role of the T-cell repertoire in the antitumor response, we next sought to assess the relationship between the TCR repertoire and clinicopathologic features of these patients. Neither T-cell density nor clonality was found to be associated with patient age, gender, smoking status, stage, presence of specific mutations, tumor size, or recurrence, though our cohort size may have limited the power to detect these associations. However, a higher level of TCR ITH (i.e., low mean MOI) was observed in older patients (Fig. 4A). Furthermore, comparison of the branch predicted MHC I and MHC II neoantigen burden to MOI revealed a negative correlation (Fig. 4B). We then compared genomic and TCR metrics across all 45 tumor regions and detected a weak negative correlation between T-cell entropy and high-affinity predicted MHC I neoantigen burden (Supplementary Fig. S9). Taken together, these data suggest that more complex genomic ITH is associated with more complex TCR ITH.

Considering the association between branch mutations and patient relapse observed in our prior study, we then compared the ITH observed in the T-cell repertoire within every tumor based on patient relapse. As shown in Supplementary Fig. S10A, a higher ITH in T-cell clonality was observed in patients who relapsed. This was further visible when patients were separated by high versus low clonality ITH, revealing

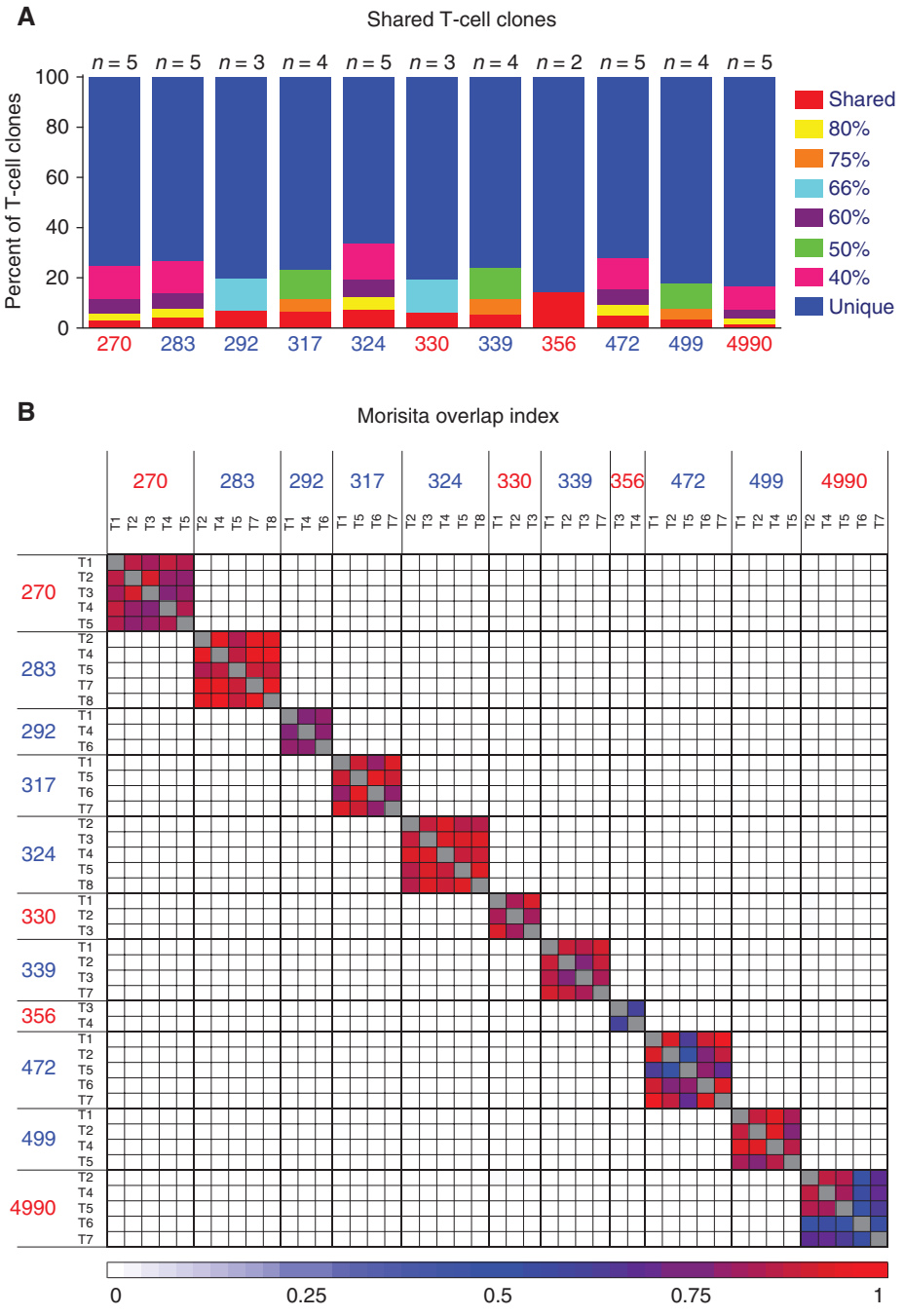

Figure 3. Substantial T-cell repertoire ITH in localized lung adenocarcinomas. **A,** Proportion of T-cell clones detected in all regions of tumors (red, shared), in 80% (yellow), in 75% (orange), in 66% (teal), in 60% (purple), in 50% (green), in 40% (pink), or restricted to a single region within the tumor (blue). **B,** Quantification of TCR ITH by comparing distinct tumor regions. The color scales indicate the MOI between 2 tumor regions. Red patient IDs = patients who relapsed; blue patient IDs = patients who have not relapsed.

that patients ≥ median showed more rapid progression (Supplementary Fig. S10A). We next compared the MOI based on patient relapse, and observed that relapsed patients had a significantly higher degree of TCR ITH (i.e., lower MOI; Fig. 4C). We then divided patients based on median MOI and evaluated disease-free survival (DFS) to see how this may relate to TCR heterogeneity. This analysis revealed a significantly longer DFS in patients with a greater than median MOI compared with those below the median (Fig. 4D). Interestingly, no significant associations to relapse were observed with regard to T-cell density ITH measured by either IHC or ImmunoSeq (Supplementary Fig. S10B and S10C). Importantly, trends were conserved when assessing associations between tumor-enriched T-cell repertoire metrics and patient relapse in the 8

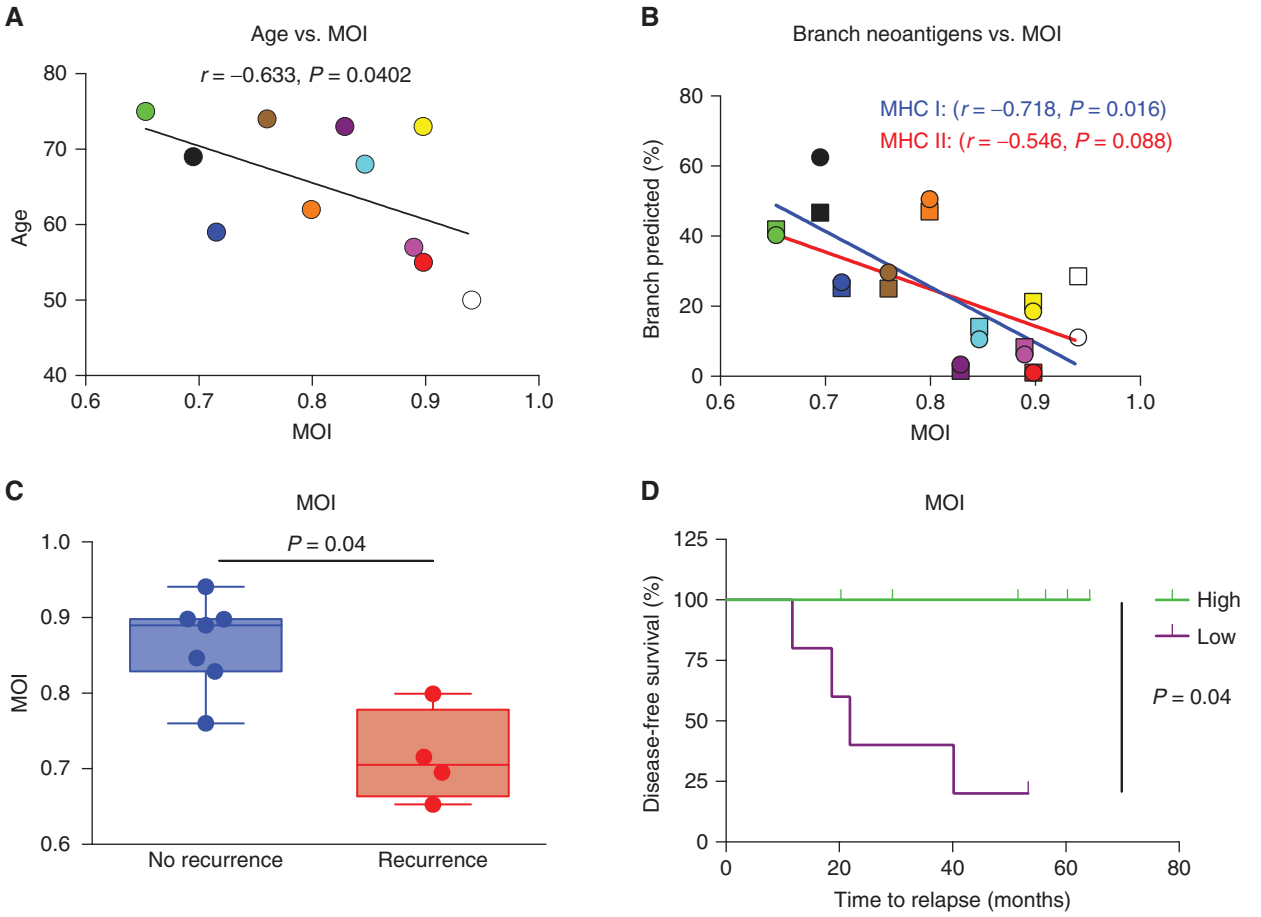

Figure 4. Correlation of T-cell repertoire ITH with clinical and genomic features of localized lung adenocarcinomas. **A,** Spearman correlation between patient age and MOI. **B,** Spearman correlation between MOI and percent predicted branch MHC I (circles, blue line) and MHC II (squares, red line) neoantigens in each patient. **C,** Recurrence status based on MOI. Red = patients who relapsed; blue = patients who have not relapsed. **D,** DFS in patients with a high (median or above, green) or low (below median, purple) MOI.

patients whose blood samples were available, though statistical significance was not attained, likely due to limited sample size (Supplementary Fig. S10D–S10F).

DISCUSSION

Recent success with immune checkpoint therapy in different cancer types has shed light on the crucial role of T cells in mediating antitumor responses (21) by highlighting their potential when efficiently targeted. In fact, all therapies exploit the potential of T cells in fighting antigen-specific targets, even as a consequence of destroying tumor cells through chemotherapy or radiotherapy (22). In addition, for patients with localized cancers undergoing surgical resection as the only treatment, elimination of potential residual micrometastases is solely dependent on the host immune system, presumably largely T cells. Therefore, studies are warranted into the role of T cells in mediating antitumor response and resistance.

Here, we performed multiregion TCR sequencing in 11 patients with localized lung adenocarcinoma in order to study the distribution of the T-cell repertoire to better understand TCR ITH and how it may relate to clinical outcomes. Our results demonstrate substantial TCR ITH in all 11 tumors in regard to infiltrating T-cell density as well as T-cell clonality. Furthermore, the extent of TCR heterogeneity was found to correlate with a patient's risk of relapse.

Our study highlights certain possibilities that could lead to emergence of T-cell repertoire ITH in NSCLC. Previous work by our group has shown that mutational heterogeneity in NSCLC, particularly an increased proportion of branch mutations, may relate to relapse in these patients (14). With recent work suggesting the importance of tumor-restricted mutations in mediating tumor immunogenicity in the form of tumor neoantigens, it is feasible that these mutations could also result in the differential intratumor expression of neoantigens and, therefore, in differences in the immunogenicity and capacity of different regions of a given tumor to induce an antitumor T-cell response. Accordingly, a recent study by McGranahan and colleagues suggested that increased ITH in the predicted neoantigen burden may be associated with patient relapse in melanoma and NSCLC, and that the best responses may be mediated by T cells responding to universally present neoantigens (15). In light of these findings, one could anticipate that any heterogeneity in the TCR repertoire

may be a result of spatial differences in abundance and nature of neoantigens within the same tumor, potentially due to heterogeneity in mutations with a unique immunogenic potential. Furthermore, the association between T-cell clonality and responses described by other groups also strengthens this possibility, as ITH was also observed in the clonality of T cells, suggesting potential differences in the response and expansion of T cells, even within a same tumor. However, we cannot exclude the possibility that the T-cell heterogeneity observed in our study may be due to heterogeneity in the architecture of these tumors, potentially within the tumor vasculature and lymphatics which could affect the capacity of T cells to traffic and infiltrate different regions of a given tumor.

Although the degree of ITH in TCR clonality and overall repertoire (as assessed by MOI) was associated with disease relapse, ITH in T-cell density by either IHC or ImmunoSeq was not. This observation may suggest that heterogeneity in the *quality* of T-cell responses may be more impactful than ITH in the *quantity* of T cells in regard to postsurgical relapse in patients with localized lung adenocarcinoma.

Because TCR sequencing was performed on bulk tumor, the T-cell subsets driving the TCR ITH observed in these tumors are unclear. However, parallel immune profiling of these samples suggested that, consistent with our previous studies (19, 20), a CD4:CD8 ratio of around 2:1 was observed in all tumors. Preliminary data from our ongoing prospective study on comprehensive immunogenomic profiling of NSCLC (ICON) also revealed similar CD4:CD8 T-cell ratios in resected NSCLC tumors using CyTOF, flow cytometry of TILs as well as IHC. The higher CD4 T-cell frequency observed could suggest heterogeneity in MHC II neoantigens could have greater implications in patient relapse. However, the limited power of current prediction algorithms due to promiscuity of MHC/peptide/TCR interactions, cellular defects in antigen processing and presentation, or even lack of immunogenicity of presented neoantigens warrants *in vitro* validation to confirm this hypothesis.

Interestingly, we observed a positive correlation between T-cell density ITH by IHC and using TCR sequencing despite that these approaches are technically different and that they were performed on nonoverlapping regions of a tumor. These analyses suggest that a single and much smaller tumor region may be sufficient to depict T-cell ITH.

Considering the potential importance of tumor heterogeneity in the mutational landscape and TCR repertoire in mediating response and resistance in NSCLC, noninvasive methods of identifying this heterogeneity in order to help predict patient response and benefit should be investigated. First, studies of peripheral T cells and circulating tumor DNA in the blood of patients are under way and may help paint a picture of the mutational and immune landscapes within the tumor. These studies may be complemented by imaging approaches, such as texture analysis, which can evaluate tumor heterogeneity using standard CT imaging (23). One could therefore anticipate that deeper analysis of the texture features of these patients' tumors may be capable of predicting ITH in the mutational landscape or in the T-cell repertoire. These studies are currently under way in a larger cohort of patients.

Finally, the heterogeneity in the mutational and TCR landscape within these patients demands investigation into approaches capable of overcoming TCR tumor heterogeneity. In addition to contributing to T-cell activation, CTLA4 blockade also helps with T-cell trafficking (24), whereas PD-1 blockade predominantly activates T cells within the tumor (21). Therefore, the possibility exists that combination of these two agents may help T cells traffic not only *to* the tumor, but *within* the tumor, and thereby promote responses by making the immune infiltrate more consistent across regions of a tumor, and therefore generating more effective antitumor responses. In addition, components of the tumor architecture may contribute to immune heterogeneity, particularly in the T-cell repertoire, which may be overcome by using chemotactic agents to improve T-cell trafficking within the tumor architecture, again promoting effective antitumor responses. Furthermore, the study by McGranahan and colleagues suggests another potential approach, in which universally present neoantigens should be targeted in order to maximize the potential for uniform T-cell responses in the tumor, with the assumption being that reactive T cells would be capable of trafficking to their targets within the tumor, unimpeded. Investigation into all these questions and others is under way in order to identify methods to target and overcome resistance mechanisms, such as tumor heterogeneity, to discover actionable mechanisms and improve responses of patients with NSCLC to therapy.

METHODS

Patients

We collected multiregion samples from 11 surgically resected lung adenocarcinomas. Informed consent was obtained from all patients. Collection and use of patient samples were approved by the Institutional Review Board of The University of Texas MD Anderson Cancer Center. Final pathologic assessment confirmed that 8 of the 11 patients had node-negative diseases, 1 patient had N2 disease (Patient #283), and 2 patients had N1 disease (Patient #270 and Patient #4990). The patient with N2 disease (Patient #283) received postoperative chemotherapy followed by radiotherapy. One of the patients with N1 disease (Patient #270) received postoperative chemotherapy with cisplatin and pemetrexed, whereas the second (Patient #4990) did not receive adjuvant chemotherapy due to comorbidities. Patient #324 received postoperative radiotherapy because of positive surgical margins. The remaining 8 patients did not receive additional therapy in the adjuvant setting. Four patients (Patients #270, #330, #356, and #4990) had disease recurrence. Clinical information is presented in Supplementary Table S1. No difference was observed in the follow-up between patients with (median follow-up, 53 months) and without (median follow-up, 42 months) recurrence (Supplementary Fig. S11).

Sample Collection and Processing for Multiregion Sequencing

Immediately after resection, 8 regions from each tumor were collected by using an 18-gauge needle core for sampling as described previously (14). A hematoxylin and eosin slide from each sample was reviewed by experienced lung cancer pathologists to assess the percentage of tumor versus normal tissues, and the percentage of malignant cells versus tumor nonmalignant stromal cells (inflammatory, vascular, and fibroblast). In addition, tumor cell viability was assessed by examining the presence of necrosis in the tissues. Only samples with at least 40% viable tumor cells were selected for DNA extraction, WES, and ImmunoSeq.

WES

The genomic data from WES were derived from our previous study (14). Sequence data have been deposited at the European Genome-phenome Archive (EGA; www.ebi.ac.uk/ega/), which is hosted by the European Bioinformatics Institute, under accession number EGAS00001000930.

Neoantigen Prediction

MHC I Neoantigens. WES data were reviewed for nonsynonymous exonic mutations (NSEM), and the binding affinity with patient-restricted MHC Class I molecules of all possible 9-mer and 10-mer peptides spanning NSEM was evaluated with the NetMHC3.4 algorithm based on patient HLA-A, HLA-B, and HLA-C alleles (25–28). Candidate peptides were considered HLA binders when $IC_{50} < 500$ nmol/L, with high-affinity binders presenting an $IC_{50} < 50$ nmol/L.

MHC II Neoantigens. WES data were reviewed for NSEM, and the binding affinity with patient-restricted MHC Class II molecules of all possible 12-mer peptides spanning NSEM was evaluated using the NetMHCIIpan3.1 algorithm (29) based on HLA-DP, HLA-DQ, and HLA-DR molecules. PHLAT was used to predict HLA typing (30), which can predict only HLA-DR and HLA-DQ. Therefore, HLA-DP was not used for MHC II prediction.

Expressed Neoantigens. Expression data for 515 normalized RNA-sequencing samples were downloaded from the Broad GDAC website (http://gdac.broadinstitute.org/runs/stddata__latest/samples_report/LUAD.html; ref. 18). Genes were then split in the TCGA dataset into low and high expression using the median value of expression profiles in the genome-wide scale as a cutoff. Among 3,962 mutated genes in our dataset associated with neoantigen prediction, 2,028 were classified into the high-expression group. Only predicted neoantigens derived from those 2,028 genes were used to test for expressed trunk and branch neoantigens and were then termed expressed neoantigens.

Trunk neoantigens were described as predicted in all tested regions of a tumor, with branch neoantigens not predicted in all regions.

TCR Sequencing

Immunosequencing of the CDR3 regions of human TCRβ chains was performed using the ImmunoSEQ Assay (Adaptive Biotechnologies). DNA remaining from WES (14) was amplified in a bias-controlled multiplex PCR, followed by high-throughput sequencing. Sequences were collapsed and filtered in order to identify and quantitate the absolute abundance of each unique TCRβ CDR3 region for further analysis, as previously described (31–34). T-cell clonality was defined as 1-Peilou's evenness and was calculated on productive rearrangements by:

$$1+\frac{\sum_{i}^{N} p_i \log_2(p_i)}{\log_2(N)}$$

where p_i is the proportional abundance of rearrangement i, and N is the total number of rearrangements (31–34).

Difference in T-cell density, unique rearrangements, and clonality within samples were calculated as the difference between the highest and lowest values in a tumor, expressed as a percentage of the highest value [(max–min)/max × 100].

MOI is a measure of the similarity in the T-cell repertoire between samples ranging from 0 to 1, taking into account the specific rearrangements and their respective frequencies, with an MOI of 1 being an identical T-cell repertoire.

Enriched T-cell rearrangements were calculated by comparing the peripheral T-cell repertoire in 8 patients with available blood to the tumor T-cell repertoire. Subsequent analyses were performed only on significantly enriched T-cell rearrangements within the tumor.

IHC

One 1 cm^2 formalin-fixed paraffin-embedded (FFPE) tumor tissue block from each patient (except Patient #324, whose FFPE block was not available) was used for immune staining with antibodies to CD3, CD4, and CD8. Four-micron-thick slides were cut from all FFPE blocks and mounted onto slides for IHC staining. Slides were then stained with CD3 polyclonal (1:100, DAKO), CD4 clone 4B12 (1:80, Leica Biosystems), and CD8 clone C8/144B (1:25, Thermo Scientific). Slides were stained using an optimized protocol using an automated IHC stainer and detected using diaminobenzidine as a chromogen and the Leica Bond Polymer Refine detection Kit (Leica Biosystems). Counterstaining was performed with hematoxylin, and slides were scanned using an automated slide scanner (Aperio AT2, Leica Biosystems) and analyzed using the Aperio Image Toolbox analysis software (Leica Biosystems). Quantification was performed by selecting 5 × 1 mm^2 regions within the tumor and measuring the average density as a count of positive cells/mm^2. Difference in T-cell density within samples was calculated as the difference between the highest and lowest values in a tumor, expressed as a percentage of the highest value [(max–min)/max × 100]. Ratio between CD4 and CD8 T cells was calculated as the average of the ratio in each of the 5 regions analyzed per sample.

Statistical Analysis

Graphs were generated with GraphPad Prism 6.0. Spearman's rank correlations were calculated to assess association between 2 continuous variables. Nonparametric Mann–Whitney *U* tests were run when comparing the recurrence and nonrecurrence groups. Kruskal–Wallis tests were used for categorical variables with more than 2 levels. *P* values were obtained using the log-rank test and the Kaplan–Meier method for estimation of DFS and overall survival.

Disclosure of Potential Conflicts of Interest

M. Vignali has ownership interest (including patents) in Adaptive Biotechnologies. S. Benzeno has ownership interest (including patents) in Adaptive Biotechnologies. D.L. Gibbons reports receiving a commercial research grant from Janssen and is a consultant/advisory board member for AstraZeneca. J.A. Wargo has received honoraria from the speakers bureaus of AstraZeneca, Bristol-Myers Squibb, and Dava Oncology, and is a consultant/advisory board member for GlaxoSmithKline, Novartis, and Roche/Genentech. H. Robins has ownership interest (including patents) in Adaptive Biotechnologies. No potential conflicts of interest were disclosed by the other authors.

Authors' Contributions

Conception and design: S. Benzeno, S. Swisher, H. Robins, P.A. Futreal, I.I. Wistuba, J. Zhang

Development of methodology: J. Zhang, J. Rodriguez-Canales, C. Gumbs, S. Benzeno, S. Swisher, H. Robins, I.I. Wistuba

Acquisition of data (provided animals, acquired and managed patients, provided facilities, etc.): A. Reuben, R. Emerson, V. Gopalakrishnan, J. Rodriguez-Canales, L.D. Little, C. Gumbs, C. Behrens, S. Benzeno, B. Sepesi, D.L. Gibbons, W.N. William Jr., S. Swisher, J.V. Heymach, P. Sharma, I.I. Wistuba, J. Zhang

Analysis and interpretation of data (e.g., statistical analysis, biostatistics, computational analysis): A. Reuben, R. Gittelman, J. Gao, J. Zhang, E.C. Yusko, C.-J. Wu, R. Emerson, J. Zhang, C. Tipton, J. Li, K. Quek, R. Chen, L.M. Vence, M. Vignali, E.R. Parra, S. Benzeno, W.N. William Jr., S. Swisher, J.J. Lee, P. Sharma, I.I. Wistuba, J. Zhang

Writing, review, and/or revision of the manuscript: A. Reuben, R. Gittelman, J. Gao, J. Zhang, E.C. Yusko, V. Gopalakrishnan, R. Chen, T. Cascone, M. Vignali, J. Fujimoto, E.R. Parra, M.-A. Forget, L. Federico, C. Haymaker, S. Benzeno, C. Bernatchez, B. Sepesi, J.A. Wargo, W.N. William Jr., S. Swisher, J.V. Heymach, J.J. Lee, P. Sharma, J.P. Allison, P.A. Futreal, I.I. Wistuba, J. Zhang
Administrative, technical, or material support (i.e., reporting or organizing data, constructing databases): V. Gopalakrishnan, M. Vignali, J. Fujimoto, J.V. Heymach, J.P. Allison, I.I. Wistuba
Study supervision: I.I. Wistuba, J. Zhang

Grant Support

This study was supported by the MD Anderson Lung Cancer Moon Shot Program, the MD Anderson Physician Scientist Program, a Conquer Cancer Foundation Young Investigator Award, a Khalifa Scholar Award, an NIH CCSG Award (CA016672), the Cancer Prevention and Research Institute of Texas (R120501), the Cancer Prevention and Research Institute of Texas Multi-Investigator Research Award grant (RP160668), The University of Texas (UT) Systems Stars Award (PS100149), the Welch Foundation Robert A. Welch Distinguished University Chair Award (G-0040), a Department of Defense PROSPECT grant (W81XWH-07-1-0306), the UT Lung Specialized Programs of Research Excellence Grant (P50CA70907), the MD Anderson Cancer Center Support Grant (CA016672), the T.J. Martell Foundation, and the Kimberley Clarke Foundation Award for Scientific Achievement through MD Anderson's Odyssey Fellowship Program.

The costs of publication of this article were defrayed in part by the payment of page charges. This article must therefore be hereby marked *advertisement* in accordance with 18 U.S.C. Section 1734 solely to indicate this fact.

Received March 9, 2017; revised June 1, 2017; accepted July 19, 2017; published OnlineFirst July 21, 2017.

REFERENCES

1. Hodi FS, O'Day SJ, McDermott DF, Weber RW, Sosman JA, Haanen JB, et al. Improved survival with ipilimumab in patients with metastatic melanoma. N Engl J Med 2010;363:711–23.
2. Topalian SL, Hodi FS, Brahmer JR, Gettinger SN, Smith DC, McDermott DF, et al. Safety, activity, and immune correlates of anti-PD-1 antibody in cancer. N Engl J Med 2012;366:2443–54.
3. Brahmer JR, Tykodi SS, Chow LQ, Hwu WJ, Topalian SL, Hwu P, et al. Safety and activity of anti-PD-L1 antibody in patients with advanced cancer. N Engl J Med 2012;366:2455–65.
4. Borghaei H, Paz-Ares L, Horn L, Spigel DR, Steins M, Ready NE, et al. Nivolumab versus docetaxel in advanced nonsquamous non-small-cell lung cancer. N Engl J Med 2015;373:1627–39.
5. Robert C, Schachter J, Long GV, Arance A, Grob JJ, Mortier L, et al. Pembrolizumab versus ipilimumab in advanced melanoma. N Engl J Med 2015;372:2521–32.
6. Rosenberg JE, Hoffman-Censits J, Powles T, van der Heijden MS, Balar AV, Necchi A, et al. Atezolizumab in patients with locally advanced and metastatic urothelial carcinoma who have progressed following treatment with platinum-based chemotherapy: a single-arm, multicentre, phase 2 trial. Lancet 2016;387:1909–20.
7. Ribas A, Kefford R, Marshall MA, Punt CJ, Haanen JB, Marmol M, et al. Phase III randomized clinical trial comparing tremelimumab with standard-of-care chemotherapy in patients with advanced melanoma. J Clin Oncol 2013;31:616–22.
8. Robert C, Thomas L, Bondarenko I, O'Day S, Weber J, Garbe C, et al. Ipilimumab plus dacarbazine for previously untreated metastatic melanoma. N Engl J Med 2011;364:2517–26.
9. Topalian SL, Sznol M, McDermott DF, Kluger HM, Carvajal RD, Sharfman WH, et al. Survival, durable tumor remission, and long-term safety in patients with advanced melanoma receiving nivolumab. J Clin Oncol 2014;32:1020–30.
10. Wolchok JD, Kluger H, Callahan MK, Postow MA, Rizvi NA, Lesokhin AM, et al. Nivolumab plus ipilimumab in advanced melanoma. N Engl J Med 2013;369:122–33.
11. Ansell SM, Lesokhin AM, Borrello I, Halwani A, Scott EC, Gutierrez M, et al. PD-1 blockade with nivolumab in relapsed or refractory Hodgkin's lymphoma. N Engl J Med 2015;372:311–9.
12. Patel SP, Kurzrock R. PD-L1 expression as a predictive biomarker in cancer immunotherapy. Mol Cancer Ther 2015;14:847–56.
13. Herbst RS, Soria JC, Kowanetz M, Fine GD, Hamid O, Gordon MS, et al. Predictive correlates of response to the anti-PD-L1 antibody MPDL3280A in cancer patients. Nature 2014;515:563–7.
14. Zhang J, Fujimoto J, Zhang J, Wedge DC, Song X, Zhang J, et al. Intratumor heterogeneity in localized lung adenocarcinomas delineated by multiregion sequencing. Science 2014;346:256–9.
15. McGranahan N, Furness AJ, Rosenthal R, Ramskov S, Lyngaa R, Saini SK, et al. Clonal neoantigens elicit T cell immunoreactivity and sensitivity to immune checkpoint blockade. Science 2016;351:1463–9.
16. Tumeh PC, Harview CL, Yearley JH, Shintaku IP, Taylor EJ, Robert L, et al. PD-1 blockade induces responses by inhibiting adaptive immune resistance. Nature 2014;515:568–71.
17. Cha E, Klinger M, Hou Y, Cummings C, Ribas A, Faham M, et al. Improved survival with T cell clonotype stability after anti-CTLA-4 treatment in cancer patients. Sci Transl Med 2014;6:238ra70.
18. Cancer Genome Atlas Research Network. Comprehensive molecular profiling of lung adenocarcinoma. Nature 2014;511:543–50.
19. Parra ER, Behrens C, Rodriguez-Canales J, Lin H, Mino B, Blando J, et al. Image analysis-based assessment of PD-L1 and tumor-associated immune cells density supports distinct intratumoral microenvironment groups in non-small cell lung carcinoma patients. Clin Cancer Res 2016;22:6278–89.
20. Federico L, Haymaker C, Forget M-A, Vence L, Team I, Sharma P, et al. P1.05–028 phenotypic and functional profiling of tumor-infiltrating lymphocytes (TIL) in early stage non-small cell lung cancer (NSCLC). J Thorac Oncol 2017;12:S630–S631.
21. Sharma P, Allison JP. The future of immune checkpoint therapy. Science 2015;348:56–61.
22. Galluzzi L, Senovilla L, Zitvogel L, Kroemer G. The secret ally: immunostimulation by anticancer drugs. Nat Rev Drug Discov 2012;11:215–33.
23. Ng F, Kozarski R, Ganeshan B, Goh V. Assessment of tumor heterogeneity by CT texture analysis: can the largest cross-sectional area be used as an alternative to whole tumor analysis? Eur J Radiol 2013;82:342–8.
24. Quezada SA, Peggs KS, Curran MA, Allison JP. CTLA4 blockade and GM-CSF combination immunotherapy alters the intratumor balance of effector and regulatory T cells. J Clin Invest 2006;116:1935–45.
25. Lundegaard C, Lamberth K, Harndahl M, Buus S, Lund O, Nielsen M. NetMHC-3.0: accurate web accessible predictions of human, mouse and monkey MHC class I affinities for peptides of length 8–11. Nucleic Acids Res 2008;36:W509–12.
26. Lundegaard C, Lund O, Nielsen M. Accurate approximation method for prediction of class I MHC affinities for peptides of length 8, 10 and 11 using prediction tools trained on 9mers. Bioinformatics 2008;24:1397–8.
27. Nielsen M, Lundegaard C, Blicher T, Lamberth K, Harndahl M, Justesen S, et al. NetMHCpan, a method for quantitative predictions of peptide binding to any HLA-A and -B locus protein of known sequence. PLoS One 2007;2:e796.
28. Shukla SA, Rooney MS, Rajasagi M, Tiao G, Dixon PM, Lawrence MS, et al. Comprehensive analysis of cancer-associated somatic mutations in class I HLA genes. Nat Biotechnol 2015;33:1152–8.
29. Andreatta M, Karosiene E, Rasmussen M, Stryhn A, Buus S, Nielsen M. Accurate pan-specific prediction of peptide-MHC class II binding affinity with improved binding core identification. Immunogenetics 2015;67:641–50.
30. Bai Y, Ni M, Cooper B, Wei Y, Fury W. Inference of high resolution HLA types using genome-wide RNA or DNA sequencing reads. BMC Genomics 2014;15:325.

31. Robins HS, Campregher PV, Srivastava SK, Wacher A, Turtle CJ, Kahsai O, et al. Comprehensive assessment of T-cell receptor beta-chain diversity in alphabeta T cells. Blood 2009;114:4099–107.
32. Carlson CS, Emerson RO, Sherwood AM, Desmarais C, Chung MW, Parsons JM, et al. Using synthetic templates to design an unbiased multiplex PCR assay. Nat Commun 2013;4:2680.
33. Robins H, Desmarais C, Matthis J, Livingston R, Andriesen J, Reijonen H, et al. Ultra-sensitive detection of rare T cell clones. J Immunol Methods 2012;375:14–9.
34. Kirsch I, Vignali M, Robins H. T-cell receptor profiling in cancer. Mol Oncol 2015;9:2063–70.